



## Perspective

## Performance and potential of porous carbons derived of electrospun metal–organic frameworks for supercapacitor applications

Petra Ágota Szilágyi, Ana Jorge Sobrido \*

School of Engineering and Materials Science, Queen Mary University of London, London E1 4NS, UK

## ARTICLE INFO

## Article history:

Received 17 December 2021

Revised 15 June 2022

Accepted 15 June 2022

Available online 21 June 2022

© 2022 Science Press and Dalian Institute of Chemical Physics, Chinese Academy of Sciences. Published by ELSEVIER B.V. and Science Press. This is an open access article under the CC BY license (<http://creativecommons.org/licenses/by/4.0/>).

## Keywords:

Electrospinning

MOFs

Porous carbons

Supercapacitors

Electrodes

Energy storage

Supercapacitors (SCs) are energy storage devices with the ability to charge and discharge at very high rates. The fast accumulation and release of charges occurs either electrostatically or electrochemically. There are two types of capacitors: electric double layer capacitors (EDLCs) and pseudocapacitors. EDLCs are the most commercially available. This type of SCs can store electrical energy *via* the reversible adsorption of the ions present in an electrolyte onto porous carbon electrodes, resulting in the formation of an electric double layer at the electrode/electrolyte interface (Fig. 1a). Although EDLCs benefit from fast kinetics, one of their main drawbacks is their cost relative to their energy density, associated with the steps involved in the production of the carbon electrodes [1]. Pseudocapacitors, on the other hand, are found somewhere in between batteries and EDLCs, as they combine faradaic redox processes and electric double layer to quickly store and release energy, leading to both higher power output and energy density than batteries and EDLCs, respectively. However, pseudocapacitors require the use of non-abundant metal oxide electrodes [2]. Organic-based pseudocapacitors have been explored as a more sustainable alternative, with recent promising results [3].

Since the capacitance is proportional to the active surface area of porous carbon, one of the obvious primary requirements for SC electrodes is a large specific surface area. High electric conductivity, hierarchical porosity and abundant active sites are also

desirable features that will contribute to the good performance of the electrode. Therefore, extensive research has been developed around the design of porous carbons with suitable pore size distributions and good electrolyte accessibility. In particular, it has been found that the charge storage in EDLCs can be maximized if the pore size is close to the size of the unsolvated electrolyte ion, which results in the ions being forced to enter the pores by the electric field losing their solvation shell. As the ions lose their solvation shell, the electrostatic interaction between electrode and ions gets stronger, resulting in an increase of the capacitance, making micro- ( $d < 2$  nm) and ultramicroporous ( $d < 1$  nm) materials ideal for SCs (Fig. 1b). Therefore, microporous have been shown to control the electrical double-layer capacitance while mesopores and macropores provide ion transport pathways and ion reservoirs, respectively [5–8]. In fact, the pore size and its distribution, rather than the particle geometry, are the primordially dominant factors in determining the performance [9]. Kornyshev et al. [10] have also analyzed this question thoroughly, reaching the following conclusions: (i) for a given voltage, there exists an optimum pore size for maximizing energy density, this ranges between *ca.* 0.8 and 1.5 nm with optima becoming increasingly closer to one another as the working voltage increases; (ii) narrower pore size distribution may result in constant specific capacitance, i.e. the practical smearing of the pore size dependence of the capacitance.

The presence of heteroatoms (e.g. N, P, S) embedded in the carbon framework can contribute significantly to performance and increase the electrolyte wettability [11]. Porous carbon materials are usually obtained by carbonization of biomass, but also coal or

\* Corresponding author.

E-mail address: [a.sobrido@qmul.ac.uk](mailto:a.sobrido@qmul.ac.uk) (A.J. Sobrido).

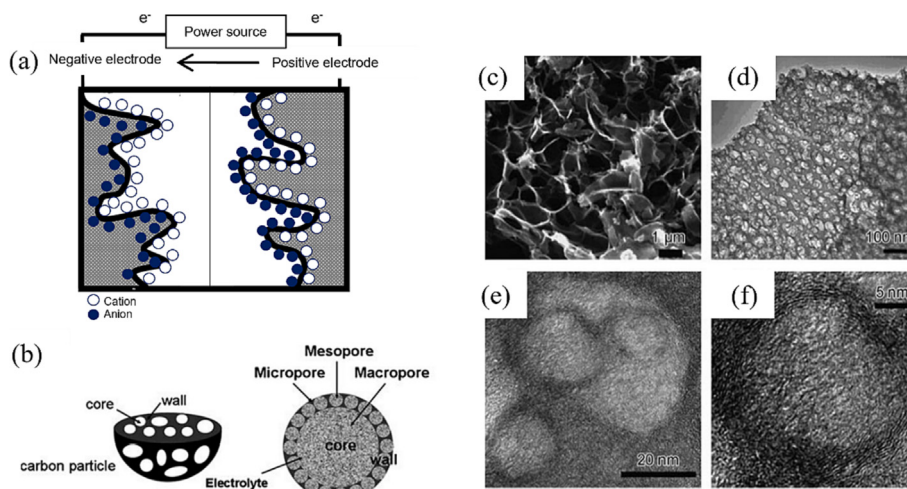


**Fig. 1.** (a) Schematic representation of the charge state in an electric double layer capacitor (EDLC). (b) Representation of 3D hierarchical porous texture. (c) SEM image of the macropores of hierarchical porous graphitic carbon, (d) TEM image of mesoporous walls, (e) TEM image showing micropores, (f) HRTEM image of localized graphitic mesopore walls. Adapted from Ref. [4] with permission from WILEY-VCH Verlag.

polymers that are then activated via a post-treatment using steam, KOH,  $\text{CuCl}_2$  or  $\text{KMnO}_4$ . While commercial SC electrodes consist of a carbon film containing the porous carbon, conductive additive and binder deposited onto a metallic current collector, three-dimensional carbon frameworks offer new opportunities in the design of novel architectures tailor-made for promoting electrochemical performance that are also self-supporting, avoiding the need of preparing a slurry to coat onto a current collector. An additional intrinsic advantage of 3D carbons is their ability to easily build hierarchical porous structures that can both enhance ion-accessible surface area and ion diffusion. Among the different strategies, electrospinning has gained interest over the last few years due to its versatility and scalability. Electrospun nanofibers have emerged as a new generation of electrodes applied to a wide range of energy storage and conversion devices, including SCs [12,13]. Electrospinning is able to produce carbon structures with different fiber diameters, surface functional groups and pore structures. Kim et al. first reported the application of electrospun carbon fibers to the development of supercapacitor devices [14]. The fibers were fabricated using poly(acrylonitrile) solutions in dimethylformamide, followed by steam activation. Maximum specific capacitances of  $173 \text{ F g}^{-1}$  and  $120 \text{ F g}^{-1}$  were obtained at  $10 \text{ mA g}^{-1}$  and  $1000 \text{ mA g}^{-1}$ , respectively. The authors attributed the maximum specific capacitance at a low current density to the micropores, while the elevated volume fraction of mesopores was responsible for the maximum capacitance value at higher current densities. In recent years, the use of biomass (lignin and cellulose, mostly) as a carbon source to produce electrospun fibers has gained increasing interest, due to the obvious benefit of using natural resources, and multiple examples of biomass-derived electrospun carbons for SCs can be found in the literature [15,16]. Biomass-derived carbons offer wide availability and low-cost, but they can also be processed into a variety of morphologies and provide a wide range of chemical features, including  $-\text{NH}_2$ ,  $-\text{COOH}$  or  $-\text{OH}$  functional groups. However, translating the requirements of the raw biomass to transform into functional energy materials and the lack of reproducibility, which depends on the origin of the biomass, remain a challenge.

Any electrospinning set-up requires three main components: (1) a supply or feed and charging the spinning solution, (2) a high-voltage power supply to generate the large potential field required, and (3) a metallic collector to deposit the electrospun fibers onto. The spin dope feed and spinneret charging generate

an elongated droplet at the tip of the needle. This elongated droplet is called the Taylor cone, and the large electric field between the spinneret and the metallic collector draws the polymer out, spinning it into small fibers onto the collector (Fig. 2a). The flexibility of this technique arises from the different experimental parameters that can be modified to alter the diameter, arrangement, texture and chemistry of the resulting fibers. These parameters include flow rate, field potential, distance of the spinning solution to the collector, collector temperature, atmosphere, spinning solution composition, inclusion of highly conducting additives, nozzle width, collector type, as well as post-treatments: activation conditions, thermal treatment to control the degree of graphitization, or surface decoration, all of which can lead to the enhancement of the electrochemical capacitance. However, there are still a few challenges electrospun materials must overcome, mainly related to reproducibility of pores of  $0.5\text{--}2 \text{ nm}$  size range and relatively low density of the fibers. Despite this, electrospun carbon electrodes have already shown remarkable performances, with capacitance values of  $\sim 150\text{--}200 \text{ F g}^{-1}$ . The density of fibers within the electrodes may be improved using sequential and concurrent electrospinning approaches, both of these techniques should be applicable for the electrospinning of MOF materials [17,18]. On the other hand, the porosity of electrospun fiber mats is typically addressed using post-production processes, such as ultrasonic treatment [19] and gas treatment such as the use of nascent  $\text{H}_2$  derived from  $\text{NaBH}_4$  [20], both of these approaches are more invasive and potentially would interfere with the MOF integrity and its interaction with the fiber mat negatively.

Furthermore, a broad variety of new chemistries and surface functionalities can be incorporated into electrospun fibers to enhance their capacity, as well as to produce greater microporous volume. Large specific surface areas will accelerate ion transport through the porous carbon electrodes, improving storage capacity and charge/discharge kinetics. One can generate different types of pores or cavities in electrospun porous carbons: inter-fiber distance ( $\sim 100 \text{ nm}$ ), mesopores ( $2\text{--}50 \text{ nm}$ ) and micropores ( $<2 \text{ nm}$ ) (Fig. 2b). The size and volume of the large inter-fiber space determines the bulk density of the electrospun fibers, and it affects the ion diffusion pathways in the electrode, so its optimization will lead to improved rate capacity. Mesopores and micropores are formed within the fiber structure and also have a significant impact on the performance of the carbon electrodes. Some of the strategies employed to increase the porosity of the fibers include

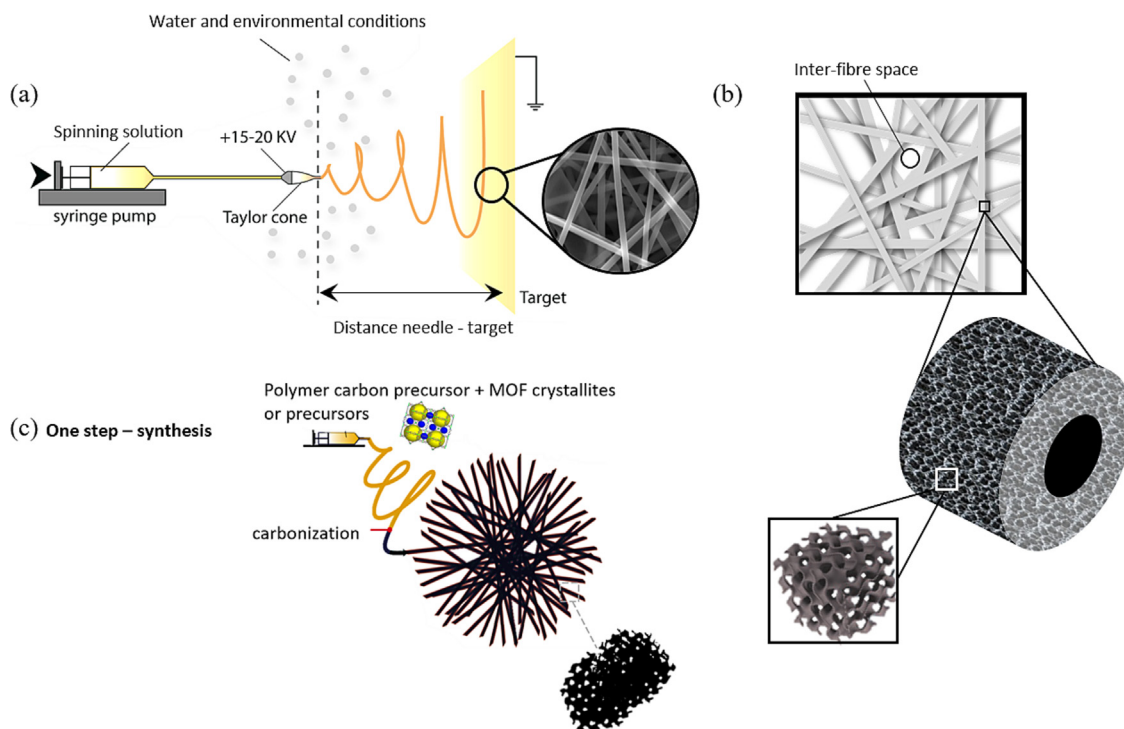


**Fig. 2.** (a) Schematic representation of the electrospinning process. (b) Different pores that can be produced in electrospun porous carbons. (c) One step synthesis to produce MOF-derived electrospun porous carbons.

conventional activation treatments like the ones applied to powdered carbons (steam, acid or alkaline activation agents) and the use of soft templates that are removed during the carbonization step.

One exciting approach that has received increasing attention is the use of metal–organic frameworks (MOFs) combined with electrospinning as precursors of porous carbons for energy and environmental applications, taking advantage of the self-templating character of MOFs [21–25]. MOFs are a class of crystalline nanostructured microporous, often ultramicroporous, materials built up of metal ions or metal oxide clusters interconnected by organic linkers, exhibiting remarkably high surface areas of several thousands of  $\text{m}^2 \text{g}^{-1}$ . MOFs are used in a variety of applications, from gas storage to catalysis or drug delivery. In fact, MOF-based electrode materials have also become a hot topic for pseudocapacitors, devices that although deliver high capacity values, undergo slower charging processes. Their tunable chemistries and pore sizes combined with the flexibility of electrospinning open a great opportunity to design a new family of hybrid materials with tailored hierarchical porosity, functionalities and active sites. Ostermann et al. [26] were the pioneers of this approach, fabricating MOF nanofibres by electrospinning a mixture of zeolitic imidazolate framework-8 (ZIF-8) and polyvinylpyrrolidone (PVP), exhibiting high porosity and tunable pore size ideal for access of electrolyte.

Various electrospinning approaches have been developed to fabricate MOF-based fiber mats. Generally speaking, they may consist of one or two consecutive steps; (i) in the formal case, *i.e.* co-electrospinning, the electrospinning mixture is typically made up of a polymer solution and MOF crystallites, or MOF precursors wherein the framework forms on electrospinning (Fig. 2c); (ii) for two-step approaches, either a pure polymer fiber mat is first electrospun onto which MOF is crystallized or MOF precursors (either linker or node) are co-electrospun with the polymer and later used as seeding sites for the growth of the MOF particles. Finally, once the MOF-based fiber mats have been obtained they may undergo

further processing, such secondary growth filling the membrane voids with additional MOF crystallites, or carbonization.

Electrospun MOF hybrids have been shown to be great candidates for SC electrodes, exhibiting high surface areas, layered porous structure and excellent capacitive performance [27]. Some examples include a nitrogen-doped nanoporous carbon fiber obtained from ZIF-8/PAN that resulted in an electrode with specific capacitance of  $332 \text{ F g}^{-1}$  and a remarkable retention rate of 98.9% after 5000 cycles at a current density of  $1 \text{ A g}^{-1}$  (Fig. 3a–f) [28]. A similar approach was employed by Chen et al. [29] to produce nitrogen-doped carbon fibers containing hollow nanoparticles from a mixture of ZIF-8 and PAN, with specific capacitance values of  $307.2$  and  $193.4 \text{ F g}^{-1}$  at  $1$  and  $50 \text{ A g}^{-1}$  current density, respectively. The electrode also showed excellent stability upon cycling with a retention rate of 98.2% after 10,000 cycles at a current density of  $5 \text{ A g}^{-1}$ . Joshi et al. used the co-electrospinning of ZIF-7 (Zn) with PAN and their subsequent carbonization to prepare freestanding electrodes for supercapacitors [30]. The specific capacity of the fibrous architecture was determined to be  $202 \text{ F g}^{-1}$  at  $1 \text{ A g}^{-1}$  current density, and 98% capacity retention was observed after 5000 charge–discharge cycles.

A step further includes the doping with B and N of the MOF-derived carbonaceous electrospun fiber-mat electrodes [31], with their best performing electrodes displaying an electrochemical capacity performance of  $295 \text{ F g}^{-1}$  at  $0.5 \text{ A g}^{-1}$  current density, and good rate capability of  $147 \text{ F g}^{-1}$  even when the current density was increased 10 times, while the cycling stability only showed a 5.5% capacitance loss over 10,000 charge–discharge cycles (Fig. 4a–g).

In a recent review by Wu et al. [32] a good summary of state-of-the-art carbon-based supercapacitor electrodes has been provided. Pristine carbon materials tend to underperform composite electrodes, with highly complex quaternary composites reported with the best performances. As a rule of thumb, the comparable electrodes, *i.e.* pure carbon and binary carbon–metal oxide electrodes

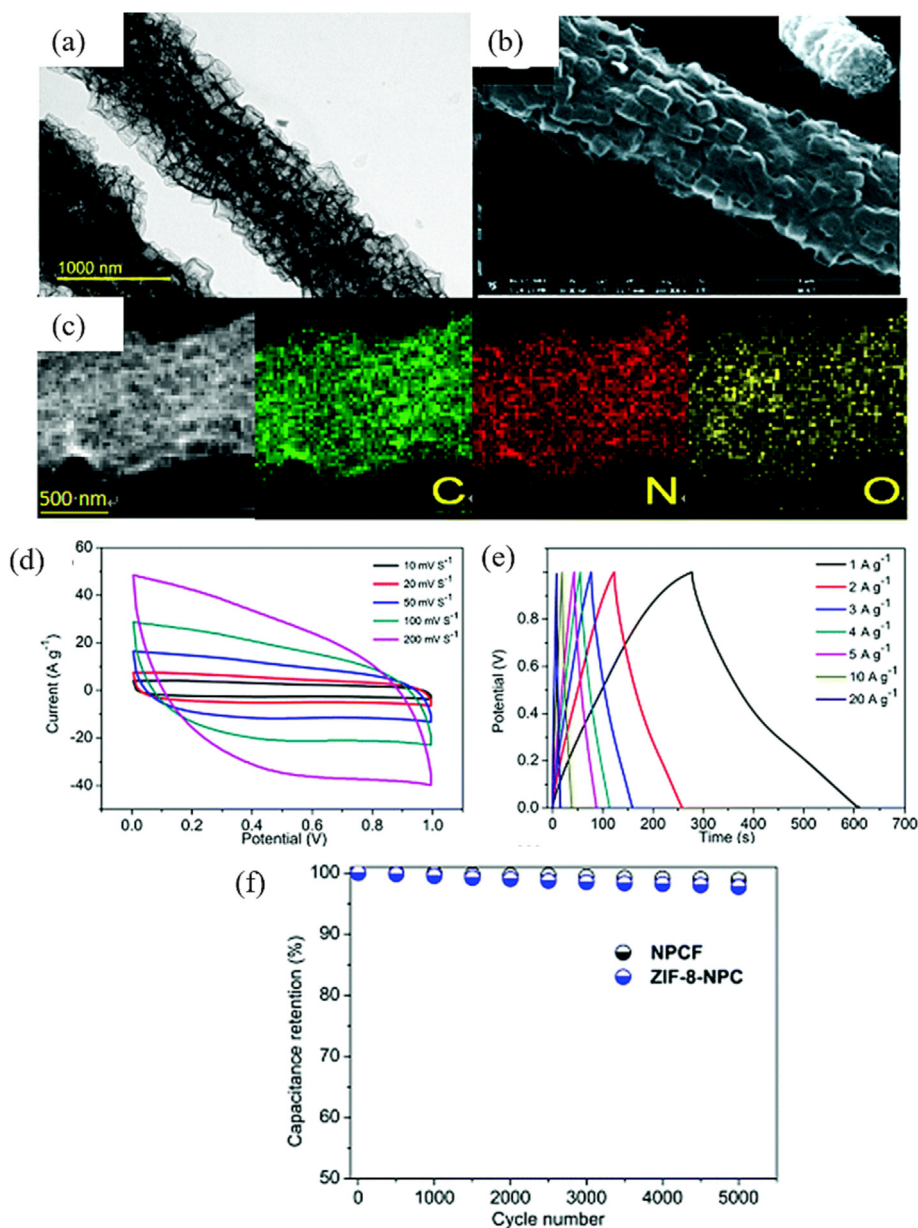


**Fig. 3.** (a) TEM and (b) SEM images of MOF-derived porous carbon fibers prepared from carbonized ZIF-8 (NPCF); (c) STEM image and corresponding element mapping of NPCF. (d and e) CV and galvanostatic charge-discharge curves of NPCF; (f) cycling performance of ZXIF-8\_NPC and NPCF measured at  $1 \text{ A g}^{-1}$  for 5000 cycles. Adapted from Ref. [28] with permission from The Royal Society of Chemistry.

typically are considered as of high performance with specific capacities in the  $250\text{--}350 \text{ F g}^{-1}$  range at  $1 \text{ A g}^{-1}$ . This is comparable with reported values for MOF-derived electrospun electrodes, where specific capacities of  $300\text{--}350 \text{ F g}^{-1}$  have been observed. Considering the novelty of this class of materials and the consequent lack of optimization both from the materials selection and processing viewpoints, it is highly likely that electrospun MOF-derived carbonaceous materials will be very strong contenders for applications as electrodes in supercapacitors. Their unique architecture offering hierarchical porosity and multitude of channels for ionic transport, combined with the variety of functionalities that also includes the presence of metals which could also provide additional pseudocapacitance, make them ideal electrode materials for supercapacitors and more work in this direction will be hopefully reported in the next years. The use of electrospinning is a fantastic addition, since it enables the production of self-

supporting fiber electrodes that can exhibit a variety of microstructural and compositional features that allow us to specifically tailor the properties of the MOF-derived carbons to produce high-performing durable EDLC electrodes.

In this Perspective, we have reviewed the opportunities offered by electrospinning metal-organic frameworks as precursors for supercapacitor applications as well as recent advances. We have argued that while this is a promising emerging approach there are still some challenges, which will have to be addressed before the technology can reach commercial maturity. Such key challenges are related to (i) controlling the morphology of the resultant fibers, particularly when upscaled; (ii) increasing the diversity of the MOF precursors in order to offer a greater variety of topologies, chemistries, and dimensionality; and, if necessary, (iii) hybridization with further additives. The morphology of both the fibers and the carbonaceous materials derived from MOFs is crucial to



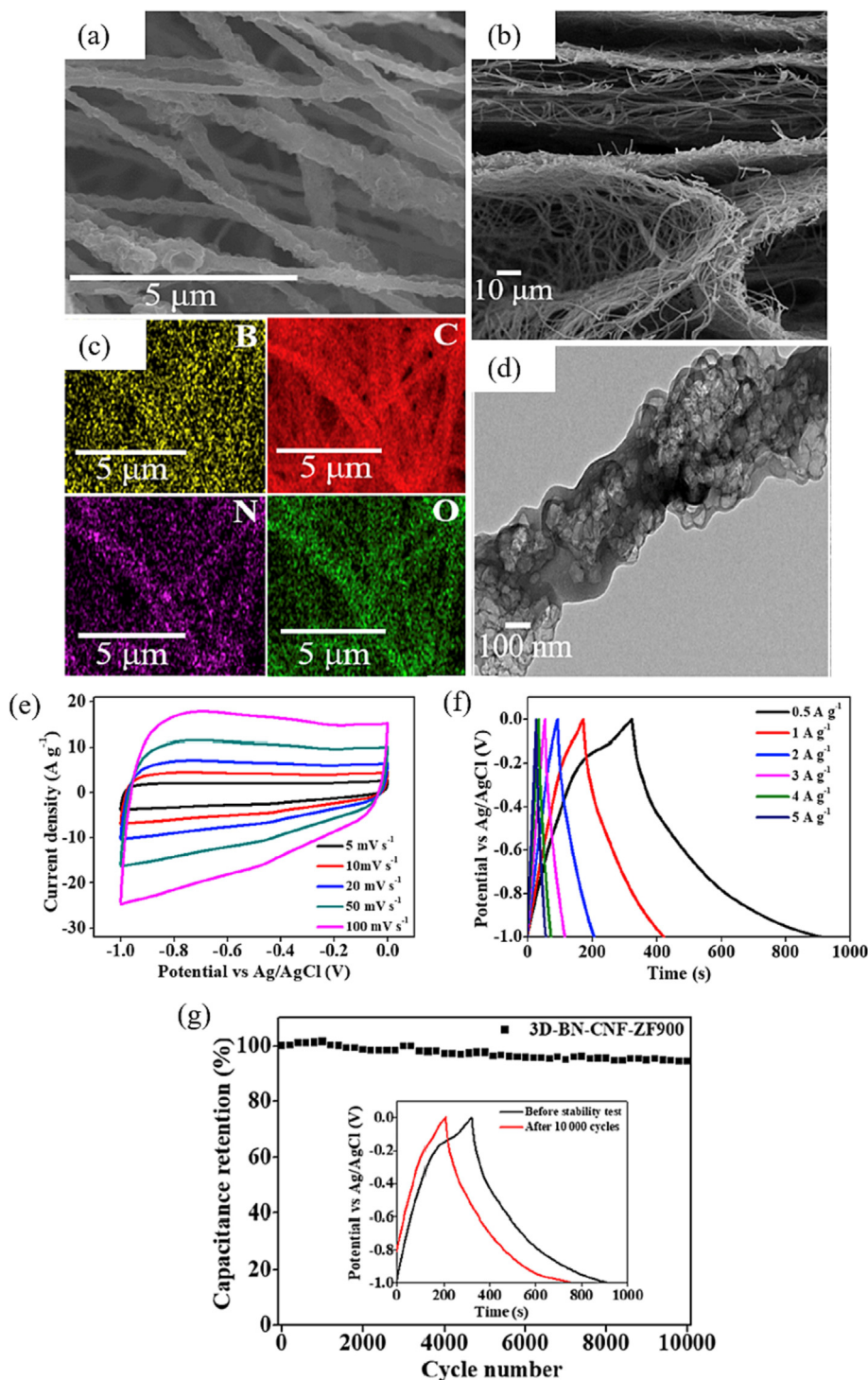


**Fig. 4.** (a) FE-SEM image of 3D-BN-CNF-ZF900, a MOF-derived carbon fibers prepared from ZIF-7; (b) cross-section view showing three-dimensionality; (c) EDS results of the distribution of the different elements present; (d) TEM image of 3D-BN-CNF-ZF900; (e) Electrochemical performances of 3D-BN-CNF-ZF900 measured in a three-electrode system with 2 M KOH as the electrolyte, (e) CV curves measured at different scan rates from 5 to 100  $\text{mV s}^{-1}$ ; (f) GCD curves at different current densities from 0.5 to 5  $\text{A g}^{-1}$ ; (g) cyclic stability test performed at 5  $\text{A g}^{-1}$  with the capacitance retention percent calculated at every 200 cycles. The inset: GCD curves before and after 10,000 cycles at 0.5  $\text{A g}^{-1}$ . Adapted from Ref. [31].

meet the requirements for high ionic transport through the hierarchical pores, in order to control this fully, further, fundamental, work is necessary to generate an understanding of the effect of carbonization conditions on the morphology of both the MOF-derived particles and the final composites. Such understanding is a must to develop scalable production. Currently, only zeolitic imidazolate

frameworks (ZIFs) have been reported as precursors for carbonaceous electrodes in supercapacitors. These frameworks are limited both in composition as well as in morphology as they form extended 3D frameworks. Typically, 2D materials afford better conductivity and therefore it is of interest to expand into the realm of 1D and 2D MOF-derived materials as well. Such an approach is

also expected to yield materials with higher electric conductivity, albeit to the detriment of the interconnected nanoporous channels, typically afforded by 3D MOFs.

Finally, further additives may provide additional electroactive sites or improved mechanical strength, adhesion, etc. Therefore, we believe that further hybridization of electrospun MOF-derived carbonaceous materials will become an area of significant development in the field.

### Declaration of competing interest

The authors declare that they have no known competing financial interests or personal relationships that could have appeared to influence the work reported in this paper.

### Acknowledgments

This work was supported by AJS's UKRI Future Leaders Fellowship (MR/T041412/1).

### References

- [1] J.R. Miller, *Science* 335 (2012) 1312–1313.
- [2] S. Fleischmann, J.B. Mitchell, R. Wang, C. Zhan, D. Jiang, V. Presser, V. Augustyn, *Chem. Rev.* 120 (2020) 6738–6782.
- [3] J.C. Russell, V.A. Posey, J. Gray, R. May, D.A. Reed, H. Zhang, L.E. Marbella, M.L. Steigerwald, Y. Yang, X. Roy, C. Nuckolls, S.R. Peurifoy, *Nat. Mater.* 20 (2021) 1136–1141.
- [4] D.-W. Wang, F. Li, M. Liu, G.Q. Lu, H.-M. Cheng, *Angew. Chem. Int. Ed.* 47 (2008) 373–376.
- [5] S. Xiong, J. Fan, Y. Wang, J. Zhu, J. Yu, Z. Hu, *J. Mater. Chem. A* 5 (2017) 18242–18252.
- [6] J. Yang, H. Wu, M. Zhu, W. Ren, Y. Lin, H. Chen, F. Pan, *Nano Energy* 33 (2017) 453–461.
- [7] Y. Fang, Q. Zhang, L. Cui, *Microporous Mesoporous Mater.* 314 (2021) 110870–110888.
- [8] R. Mendoza, J. Oliva, V. Rodriguez-Gonzalez, *Int. J. Energy Res.* 46 (2022) 6989–7020.
- [9] L. Xie, K. Yuan, J. Xu, Y. Zhu, L. Xu, N. Li, J. Du, *Front. Chem.* 8 (2020) 599981–599994.
- [10] S. Kondrat, C.R. Perez, V. Presser, Y. Gogotsi, A.A. Kornyshev, *Energy Environ. Sci.* 5 (2012) 6474–6479.
- [11] L. Miao, Z. Song, D. Zhu, L. Li, L. Gan, M. Liu, *Mater. Adv.* 1 (2020) 945–966.
- [12] J. Liang, H. Zhao, L. Yue, G. Fan, T. Li, S. Lu, G. Chen, S. Gao, A.M. Asiri, X. Sun, *J. Mater. Chem. A* 8 (2020) 16747–16789.
- [13] W. Yue, M.D.R. Kok, J.P. Victoria Tafoya, A.B. Jorge Sobrido, E. Bell, J.T. Gostick, S. Herou, P. Schlee, M.M. Titirici, D.J.L. Brett, P.R. Shearing, R. Jervis, *J. Energy Chem.* 59 (2021) 492–529.
- [14] C. Kim, K.S. Yang, *Appl. Phys. Lett.* 83 (2003) 1216–1218.
- [15] P. Schlee, S. Herou, R. Jervis, P.R. Shearing, D.J.L. Brett, D. Baker, O. Hosseinaei, P. Tomani, M. Mangir Murshed, Y. Li, M.J. Mostazo-Lopez, D. Cazorla-Amoros, A.B. Jorge Sobrido, M.M. Titirici, *Chem. Sci.* 10 (2019) 2980–2988.
- [16] I. Moulefera, M. Trabelsi, A. Mamun, L. Sabantina, *Polymers* 13 (2021) 1071–1091.
- [17] J.-S. Kim, B.G. Im, G. Jin, J.-H. Jang, *ACS Appl. Mater. Interf.* 8 (2016) 22721–22731.
- [18] K.M. Sajesh, K. Kiran, S.V. Nair, R. Jayakumar, *Compos. Part B: Eng.* 99 (2016) 445–452.
- [19] B.K. Gu, S.J. Park, M.S. Kim, C.M. Kang, J.-I. Kim, C.-H. Kim, *Carbohydr. Polym.* 97 (2013) 65–73.
- [20] J. Jiang, M.A. Carlson, M.J. Teusink, H. Wang, M.R. MacEwan, J. Xie, *ACS Biomater. Sci. Eng.* 1 (2015) 991–1001.
- [21] Y. Dou, W. Zhang, A. Kaiser, *Adv. Sci.* 7 (2020) 1902590–1902611.
- [22] X. Lu, C. Wang, F. Favier, N. Pinna, *Adv. Energy Mater.* 7 (2017) 1601301–1601344.
- [23] D. Tian, Y. Ao, W. Li, J. Xu, C. Wang, *J. Colloid Int. Sci.* 603 (2021) 199–209.
- [24] C. Wang, Y.V. Kaneti, Y. Bando, J. Lin, C. Liu, Y. Yamauchi, *Mater. Horiz.* 5 (2018) 394–407.
- [25] H.B. Wu, X.W.D. Lou, *Sci. Adv.* 3 (2017) 1–16.
- [26] R. Ostermann, J. Cravillon, C. Weidmann, M. Wiebcke, B.M. Smarsly, *Chem Commun.* 47 (2011) 442–444.
- [27] K. Mi, L. Song, H. Nie, T. Liu, X. Li, *J. Energy Chem.* 47 (2020) 221–224.
- [28] C. Wang, C. Liu, J. Li, X. Sun, J. Shen, W. Han, L. Wang, *Chem Commun* 53 (2017) 1751–1754.
- [29] L.F. Chen, Y. Lu, L. Yu, X.W. Lou, *Energy Environ. Sci.* 10 (2017) 1777–1783.
- [30] B. Joshi, S. Park, E. Samuel, H.S. Lo, S. An, M.-W. Kim, M.O. Swihart, J.M. Yun, K. H. Kim, S.S. Yoon, *J. Electroanal. Chem.* 810 (2018) 239–247.
- [31] B. Dahal, T. Mukhiya, G.P. Ojha, A. Muthurasu, S.-H. Chae, T. Kim, D. Kang, H.Y. Kim, *Electrochimica Acta* 301 (2019) 209–219.
- [32] Y. Pan, K. Xu, C. Wu, *Nanotechnol. Rev.* 8 (2019) 299–314.